Available online at www.sciencedirect.com

ScienceDirect

Procedia Structural Integrity 68 (2025) 854–860

Structural Integrity Procedia

www.elsevier.com/locate/procedia

European Conference on Fracture 2024

Multi-material laser powder bed fusion: The effect of cross-contaminations of Cu particles in AlSi10Mg feedstock on the mechanical properties of the part

Christopher Singer[a], Max Horn[a], Georg Schlick[a], Johannes Schilp[b], Saba Zabihzadeh[c], Christina-Margarita Charalampidou[d], Nikolaos D. Alexopoulos[d,*]

[a] *Fraunhofer Research Institute for Casting, Composite and Processing Technology IGCV, Am Technologiezentrum 10, 86159 Augsburg, Germany*

[b] *University of Augsburg, Chair of Digital Manufacturing, Am Technologiezentrum 8, 86159 Augsburg, Germany*

[c] *Swiss Centre for Electronics and Microtechnology (CSEM), Additive manufacturing and component reliability, Neuchâtel, Switzerland*

[d] *University of the Aegean, Department of Financial Engineering and Management, Research Unit of Advanced Materials, 82100 Chios, Greece*

Abstract

Cross-contamination after mixing metal powders in multi-material laser powder bed fusion (MMLPBF) is a common production problem and represents a significant barrier to the advancement of this emerging additive manufacturing technology. To assess the effect of such contamination on a key material combination for MMLPBF, the present article examines the effect of cross-contamination of CuCr1Zr foreign particles in AlSi10Mg feedstock on the respective metallurgical and mechanical properties of the final part. Different CuCr1Zr contamination levels were selected, e.g. of 0.5 wt.%, 3.0 wt. % and 5.0 wt.%, respectively, and the test results were compared against the uncontaminated feedstock. The metallurgical structure of CuCr1Zr contaminated samples revealed characteristic Al-rich inclusions. Tensile tests indicate that these inclusions result in material embrittlement and – in general - reduced tensile mechanical properties Quantitative analysis of the tensile test results showed that the quality (consisting of both, tensile strength and deformation capabilities) of printed samples strongly depends on both the contamination level and printing direction. The investigation discusses critical contamination levels for this material combination and explores the potential for powder reusability and in-situ alloying applications.

Keywords: laser powder bed fusion; additive manufacturing; tensile test; contamination; AlSi10Mg

* Corresponding author. Tel.: + 302271035464; fax: +302271035484.
E-mail address: nalexop@aegean.gr

2452-3216
10.1016/j.prostr.2025.06.141

1. Introduction

Multi-material laser powder bed fusion (MMLPBF) is gaining ground to address the continuous increasing demands for highly precise manufacturing of metallic components with reduced process lead time and increased sustainability. This method is particularly advantageous for industries such as aerospace and automotive, where material flexibility and complex geometries are often required. However, the metal powder cross-contamination is probably one of the most important constraints for the wide exploitation of the novel additive manufacturing technology. Even minimal cross-contamination, especially when combining dissimilar metals, can significantly impact the mechanical properties, structural integrity, and functional performance of the printed components (DebRoy, et al., 2018) (Spierings & Wegener, 2020). Additive manufacturing of bi-metals is extremely challenging in the automotive industry, where the printing of aluminium alloys on copper alloys or vice versa represents most of the use-cases in this field.

In the present work, a preliminary investigation will be performed to assess the effect of cross-contamination with CuCr1Zr foreign particles of AlSi10Mg feedstock. In the automotive sector, combining aluminum alloys with copper-based materials (e.g., CuCr1Zr) is challenging due to differences in melting points, thermal conductivities, and material compatibilities. Aluminum alloys like AlSi10Mg are widely used for their lightweight and excellent strength-to-weight ratio, whereas copper alloys contribute high thermal and electrical conductivities. The effectiveness of MMLPBF in such combinations, however, can be constrained by particle contamination, which often affects the integrity of the printed structure (Herzog, Seyda, Wycisk, & Emmelmann, 2016). Previous studies have shown that the introduction of foreign particles in the metal powder feedstock not only alters microstructural characteristics but also has adverse effects on tensile strength, ductility, and fatigue life (Horn, et al., 2019), (Mumtaz & Hopkinson, 2020). Several powder contamination grades ranging from 0.5 to 5.0 weight percent (wt. %) are processed and compared with uncontaminated powder feedstock for both cases. According to previous investigations, *e.g*., (Horn, et al., 2019), the MMLPBF samples showed different microstructures and mechanical properties, confirming the differences due to the foreign particle concentrations. The decrease in the mechanical properties for both cases was quantified and reported in terms of foreign particles concentration and consequently contamination. The tensile mechanical properties were used as an input to calculate the "quality" of the printed samples with different levels of cross-contamination. The damage tolerance quality index (Q_D) was exploited from the casting industry of aluminium alloys, *e.g*., (Alexopoulos & Pantelakis, 2004), to assess the printing quality of the MMLPBF samples. The quality index comprises of both, strength and ductility capabilities of the samples and it was associated with the investigated contamination levels. Diagrams of quality level, according to (Alexopoulos N. , 2007), along with the desired mechanical properties were plotted and the results are discussed over the contamination levels and the appropriate quality.

2. Experimental procedure

2.1. Materials

The powder materials used for the specific application of the present study, which is the production of high performance automotive – power electronics sensing / cooling as well as bus bars were Al and Cu alloys, whereas the Cu alloy could serve as functional material for electricity or heat conduction. On the contrary, the Al alloy should mainly serve as structural material and bear the main forces. Thus, in this study, the Cu contamination of Al alloy particles was investigated, and the following materials were chosen. The Cu alloy CW106C, which is referred to as CuCr1Zr, was selected to serve as contamination material. Adding Chromium (Cr) and Zirconium (Zr) to the Cu matrix increases material strength as well as heat and wear resistance without significantly affect its heat and electric conductivity capabilities. The Al alloy EN AC-43000, which is referred to as AlSi10Mg, was selected as matrix material. It is a precipitation hardenable cast alloy with good electric conductivity and increased chemical stability in corrosive environments according to (DIN EN 1706, 2013). Due to its high flexibility in laser powder bed fusion (LPBF) processes combined with high specific strength, it is currently the most common used Al alloy for this kind of additive manufacturing (AM) processes, *e.g*., (SLM Solutions , 2019). Metal powder from SLM

Solutions Group AG with +20/-63 µm clarification was used for the underlying study. Powder with a clarification of +20/-45 µm was supplied by Schmelzmetall GmbH.

2.2. Mixing of the powders

To ensure comparability with the structural defects described by (Horn, et al., 2018), the same contamination levels were selected. Since the qualitative differences between 0.5 wt.% and 1.0 wt.% were minimal, the 1.0 wt.% level was excluded from this study. Therefore, contamination levels of 0.5 wt.%, 3.0 wt.%, and 5.0 wt.% were analysed. The two powders were blended in a drum hoop mixer to homogenize the powder mixture and manually tumbled. Powder mixtures were processed on a SLM 250 HL LPBF machine from SLM Solutions Group AG.

2.3. Additive manufacturing phase

Cubes with geometrical dimension of 10 mm × 10 mm × 10 mm were printed and was used for metallographic investigation. The Reference Intensity Ratio (RIR) method was used for semi-quantitative phase identification. Additionally, at least three (3) tensile specimens were printed per different printing orientation (three different orientations were exploited, namely 0°, 45° and 90°, respectively) with regards to building direction and for the different contamination degree. The tensile specimens were manufactured in the form of rods and were afterwards machined according to DIN 50125 – B4 x 20 standards to meet the geometrical dimensions of total length l_{total} = 41 mm, reduced diameter d = 4 mm and gauge length at the reduced cross-section l_{gauge} = 20 mm.

2.4. Evaluation of additive manufactured materials

For the evaluation of the printed specimens each microstructural analysis was performed (e.g., XRD, RIR etc.) and mechanical testing. The mechanical tests included tensile testing which was performed on a UPM 50 kN machine from Zwick Roell in accordance with DIN EN ISO 6892-1. Less but not least, the mechanical test results were qualitatively analysed by employing the “quality index” concept. The “quality index” was a concept firstly proposed by (Drouzy, Jacob, & Richard, 1980) to assess the chemical composition differences in cast aluminium alloys AlSiMg as well as the foundry processing variables on the tensile mechanical behaviour of the casts. In this regard, to reduce the experimental effort as well as comprising the capabilities of the materials for tensile strength and ductility (Drouzy, Jacob, & Richard, 1980), introduced the empirical equation:

$$Q = R_m + 150 \cdot \log(A_f), \tag{1}$$

where R_m stands for the ultimate tensile strength and A_f refers to elongation at fracture. This equation includes two different terms, the first one gives information on the mechanical strength level (strength) and the second one gives information of the tensile ductility level (logarithm of elongation at fracture) to quantify in a single number the capability for tensile mechanical behaviour. The empirical term of 150 was evaluated according to numerous tests and evaluations and is considered as a constant value for A357 (AlSiMg) cast aluminium alloys.

Nevertheless, in case that such materials must be used in modern light/weight structures, they need to have high damage tolerance capabilities, i.e. the quantification of their quality should include metrics for the respective damage tolerance mechanical properties. In this regard, (Alexopoulos & Pantelakis, 2004) proposed a modified quality index that included the damage tolerance mechanical behaviour in one quantified index Q_0, multiplied by the dimensions less index K_D comprising the capability of the material for scatter in mechanical properties. Hence, the damage tolerance quality index Q_D was formed as:

$$Q_D = K_D \cdot Q_0, \tag{2}$$

where K_D stands for a dimensionless factor and Q_0 characterizes the tensile performance of the material. In analogy to Drouzy’s (Drouzy, Jacob, & Richard, 1980) quality index, this term comprises the mechanical strength and tensile ductility parts and it was formulated as their summation to form the initial mechanical quality Q_0 as:

$$Q_0 = R_p + 10 \cdot W, \tag{3}$$

where R_p refers to tensile yield stress while W to the tensile strain energy density and is calculated as the integral of the tensile stress-stain curve. This mechanical property was found to better reflect the damage tolerance characteristics of the material, as according to (Sih & Jeong, 1990) energy density may be directly related to the plain strain fracture toughness value K_{IC}, which evaluates the fracture of a cracked member under plain strain loading conditions. The empirical coefficient 10 represents a typical value of the ratio R_p / W of the already optimized aluminium alloys according to (Alexopoulos N. , 2007). Following, the K_D factor was determined as:

$$K_D = \left(\frac{R_{pi}}{R_{pmax}} + \frac{W_i}{W_{max}}\right) \leq 2 \tag{4}$$

where R_{pi} stands for the yield stress of the i specimen, R_{pmax} stands for the maximum yield stress achieved for the same test series, W_i stands for the energy density of the i specimen, and W_{max} stands for the maximum energy density achieved for the same test series.

3. Characterization of the powders

Representative pictures from the cross-contaminated powders (simulating recycled powders) are shown in Fig. 1 for the higher contamination levels investigated.

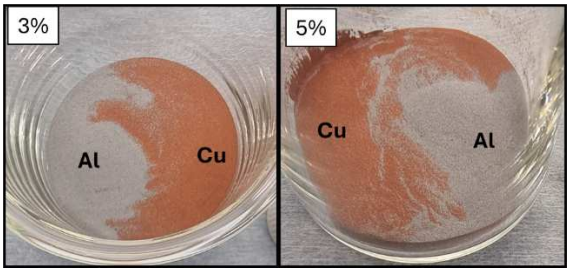

Fig. 1: Typical macro-photos of cross-contamination levels of Al and Cu powders.

Fig. 2 presents the SEM images of the powders with different contamination levels. It was noticed that the SEM micrographs confirm the presence of Cu powder cross contamination that can be seen as large diameter particles. The cross contamination is not homogeneous, and the SEM images were randomly taken. Single isolated enclosures of Al (shown in yellow colour) are distributed in the material. With increasing contamination level (*e.g.*, 3.0 wt.%) accumulation of Al enclosures in specific areas of the material (in proximity) is noticed.

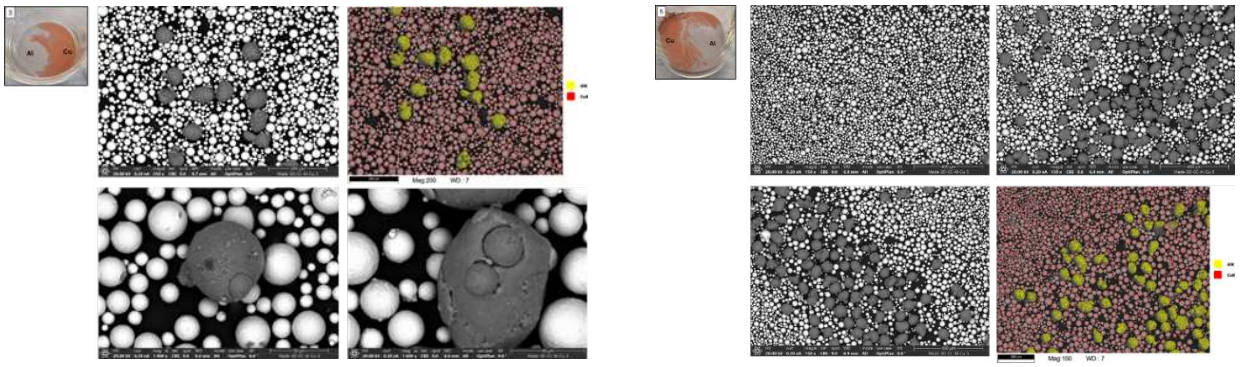

Fig. 2: SEM micrographs for the different contamination levels 3.0% wt (left) and 5.0 wt% (right).

4. Evaluation

Fig. 3 presents the effect of 0.5 wt.%, 3.0 wt.% and 5.0 wt.% contamination level of CuCr1Zr foreign particles in AlSi10Mg matrix on tensile conventional yield stress $R_{p0.2\%}$ and ultimate tensile strength R_m. All graphs show the results of the properties as average values for all three build directions (0°, 45° and 90°). As expected, cross-contamination resulted to increased conventional yield stress $R_{p0.2\%}$ for all printed directions due to phase-hardening effects. Significant increase in $R_{p0.2\%}$ was noticed with increasing contamination level for almost all printed samples. Nevertheless, a significant drop of the property was evident for inclined samples (45°) at the first stages of contamination (*e.g.*, 0.5 wt %. contamination level). The samples printed horizontally (90° to build direction) showed higher $R_{p0.2\%}$ values for the short contamination levels (0 wt.% and 0.5 wt.%). In inclined printed samples (45° to build direction) the highest $R_{p0.2\%}$ values were observed for the high contamination levels.

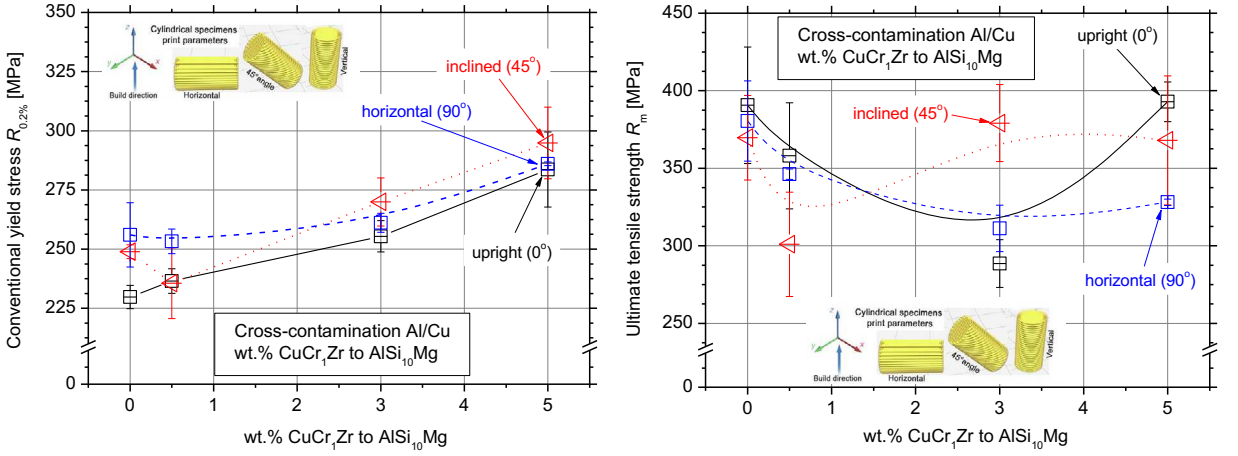

Fig. 3. Tensile test results of conventional yield stress $R_{p0.2\%}$ (left) and ultimate tensile strength R_m (right) of the investigated cross-contamination levels.

From the metallurgical point of view, in the binary Al-Cu alloying system several intermetallic phases are formed. In principle, Cu is the principal alloying element in the 2xxx series of Al alloys, enabling precipitation hardening. Up to 5.56 wt.% of Cu can be dissolved in Al-matrix, forming a solid solution. Beyond this concentration level, θ (Al_2Cu) intermetallic phase nucleates while at 53.5 wt.% Cu in Al alloys, the system is composed entirely of the θ phase. In this regard, the copper contamination can increase yield stress by either the formation of intermetallic phases, e.g. theta (θ) phase, or by solid solution strengthening of the larger in diameter Cu particles on the Al matrix. The Cu additions seem to play a different role depending on the targeting tensile mechanical property, e.g. ultimate tensile strength R_m. Fig. 3 also summarizes the ultimate tensile strength values for the different contamination levels, where it is shown that the Cu contamination decreases R_m for the low contamination levels and a R_m recovery can be noticed for specific printing orientations for the higher investigated contamination. In general, the samples printed upright (0° to build direction and in black colour) showed the higher R_m values almost for all contamination levels. An exception is noticed after 3.0 wt. % CuCr1Zr to AlSi10Mg but a recovery is noticed after the 5.0 wt. % contamination level. Additionally, for the horizontal printed samples (90° to build direction and in blue colour), the increase in contamination level led to R_m gradual decrease. Finally, the inclined printed specimens (45° to build direction and in red colour) presented better results for the high contamination levels (e.g., 3.0 wt.% and 5.0 wt.%).

On the contrary, cross-contamination had a decreasing effect on elongation at fracture A_f for all printed directions with increasing contamination level, shown in Fig. 4. The samples printed horizontally (90° to build direction) showed better A_f values for almost all contamination levels apart from the highest level (5.0 wt.%), probably due to interconnection of Cu enclosures at high contamination levels. The inclined printed samples (45° to build direction) showed the lowest values of elongation at fracture for the short contamination levels up to 0.5 wt.%, but an

improvement was noticed for higher levels. A recovery of the property was noticed after 5.0 wt.% contamination level for upright printed samples (0° to build direction).

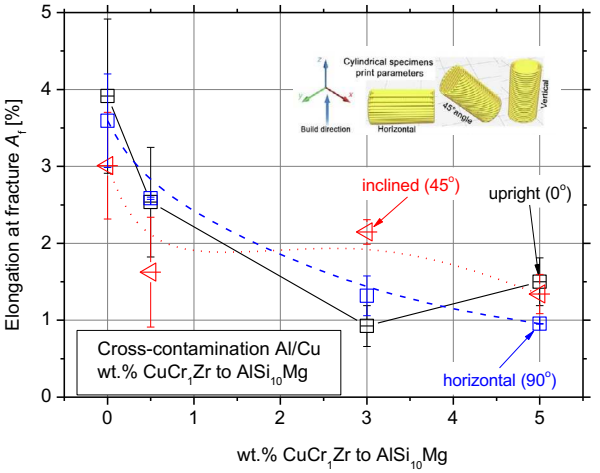

Fig. 4. Tensile elongation to fracture A_f of the investigated cross-contamination levels.

The quality index analysis comprises both, mechanical strength and tensile ductility capabilities and the results were plotted for the different cross-contaminations/printing orientations over yield stress and strain energy density axis of Fig. 5. The horizontal (90°) printing without no contamination gives the higher quality of approximate 370 MPa. The gradual increase in contamination decreases the quality in the horizontal (90°) printing and stabilizes around 300 MPa for the high cross-concentration levels investigated. The higher quality decrease was noticed for the vertical/upright (0°) printing with the gradual increase in contamination, while a recovery is noticed for the high concentration. Finally, the inclined printed samples (45° to build direction) show almost the same quality despite the contamination level (exception is the short contamination level of 0.5 wt.%). A general comment from the quality index analysis, is that for the upright and horizontal build directions, the high (5.0 wt.%) contamination level the quality is essentially decreased. This is not the case for the inclined printed specimens as the quality remains almost unaffected of the cross-contamination level, better levelling the decrease of tensile ductility over the strength increase due to the formation of intermetallic phases.

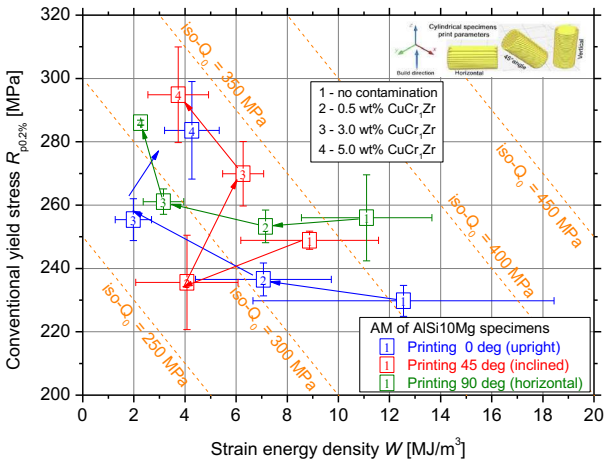

Fig. 5. Quality index analysis of the investigated cross-contamination levels and printing orientation.

4. Conclusions

A comprehensive experimental study and a qualitative analysis was conducted on the effect of cross-contamination of Al and Cu in additively manufactured specimens, regarding their microstructural characteristics and mechanical behaviour. The results of the study revealed that the phase enclosures which are formed due to the increased level of contamination led to a considerable increase in yield stress along with decrease in elongation at fracture, while the printing direction plays a key role in the mechanical behaviour, with the samples printed horizontally (90° to the build direction) presenting the best tensile test results for almost all contamination levels. The quality index of the printed samples showed a recovery after 5.0 wt.% contamination level in upright and horizontal print directions, while in inclined printed specimens remained almost unaffected of contamination level.

Acknowledgements

The authors gratefully acknowledge the financial support of the HORIZON Research and Innovation Actions, European Health and Digital Executive Agency for the implementation of the project «MULTI-MATERIAL DESIGN USING 3D PRINTING» having an acronym "MADE-3D" of the act HORIZON-CL4-2022-RESILIENCE-01 with Grant Agreement code 101091911.

References

Alexopoulos, N. D. (2007). Generation of quality maps to support material selection by exploiting the quality indices concept of cast aluminum alloys. *Materials and Design*, pp. 534-543.

Alexopoulos, N. D., & Pantelakis, S. G. (2004). A New Quality Index for Characterizing Aluminum Cast Alloys with Regard to Aircraft Structure Design Requirements. *Metallurgical and Materials Transactions A: Physical Metallurgy and Materials Science A, 35*, pp. 301-308.

DebRoy, T., Wei, H. L., Zuback, J. S., Mukherjee, T., Elmer, J. W., Milewski, J. O., & Zhang, W. (2018). Additive manufacturing of metallic components – Process, structure and properties. *Progress in Materials Science, 92*, pp. 112-224.

DIN EN 1706. (2013). Aluminium and aluminium alloys - Castings - Chemical composition and mechanical properties. Berlin, Beuth .

Drouzy, M., Jacob, S., & Richard, M. (1980). Interpretation of tensile results by means of quality index and probable yield strength. *AFS Int. Cast Metals Jnl*, pp. 43-50.

German Copper Alliance. (2010). *Cu Al Alloys.* Informationsdruck i.6.

Herzog, D., Seyda, V., Wycisk, E., & Emmelmann, C. (2016). Additive manufacturing of metals. *Acta Materialia,117*, pp. 371-392.

Horn, M., Schlick , G., Wegner , F., Seidel , C., Anstaett, C., & Reinhart, G. (2018). Defect formation and influence on metallurgical structure due to powder cross-contaminations in LPBF. *Proceedings of 7th International Conference on Additive Technologies.*

Horn, M., Schlick, G., Lutter-Guenther, M., Anstaett, C., Seidel, C., & Reinhart, G. (2019). Metal powder cross-contaminations in multi-material laser powder bed fusion: Influence of CuCr1Zr particles in AlSi10Mg feedstock on part properties. *Proceedings of the Lasers in Manufacturing Conference*, pp. 1-11.

Macherauch, E., & Zoch, H.-W. (2011). *Praktikum in Werkstoffkunde: 91 ausführliche Versuche aus wichtigen Gebieten der Werkstofftechnik.* Wiesbaden: Vieweg+Teubner.

Mumtaz, K. A., & Hopkinson, N. (2020). Selective laser melting of aluminum and copper materials for multi-material production. *Additive Manufacturing, 31*, p. 100970.

Sih, G., & Jeong, D. (1990). Fatigue load sequence effect ranked by critical available energy density. *Theoretical and Applied Fracture Mechanics, 14*, pp. 141-151.

SLM Solutions . (2019). Material Data Sheet Al-Alloy AlSi10Mg / EN AC-43000 / EN AC-AlSi10Mg, 190201 AlSi10Mg.

Spierings, A. B., & Wegener, K. (2020). Laser powder bed fusion of high-performance materials for industry applications. *Additive Manufacturing, 36*, p. 101470.